THE ASTROPHYSICAL JOURNAL, 299:845–851, 1985 December 15

SEARCH FOR SCATTERED X-RAY HALOS AROUND VARIABLE SOURCES: THE X-RAY HALO OF CYGNUS X-1

M. F. BODE[1]
Department of Astronomy, University of Manchester, and Earth and Space Sciences Division, Los Alamos National Laboratory
W. C. PRIEDHORSKY[1]
Earth and Space Sciences Division, Los Alamos National Laboratory
G. A. NORWELL
Department of Physics, University of Keele, and Earth and Space Sciences Division, Los Alamos National Laboratory
AND
A. EVANS
Department of Physics, University of Keele
Received 1985 February 13; accepted 1985 June 19

ABSTRACT

The results of a program to search for the presence of halos due to X-ray scattering by interstellar grains in the line-of-sight to variable X-ray sources are reported. As part of this program, four *Einstein* HRI images of Cyg X-1 were examined. The analysis technique exploits the intrinsic aperiodic variability of this source to map the point response function of the optics. Any scattered halo present will not reflect short-term central source time variability, since such variability is smoothed by differential time delays of order days. Thus, a residual, nonvariable component to the surface brightness distribution (comprising $\gtrsim 12\%$ of the source flux) is interpreted as a scattered halo. The Cyg X-1 halo is consistent with those of other sources found in previous studies using different techniques. Comparison is also made with a scattering model, and, despite uncertainties in source spectrum and distance, reasonable agreement with the observations is found using a standard interstellar grain model. The potential of X-ray scattering as a probe of the properties of interstellar grains is demonstrated.

Subject headings: interstellar: matter — X-rays: sources

I. INTRODUCTION

The properties of interstellar grains have been explored at wavelengths from the ultraviolet to the infrared. Such observations are beginning to give a self-consistent picture of grain composition, size, and number density distribution (see, e.g., Whittet 1981 and references therein). Overbeck (1965) first pointed out that grains will also be sites of scattering at X-ray wavelengths. Hayakawa (1970) and Martin (1970) further explored this possibility and suggested that not only would such effects be readily detectable with suitable imaging telescopes, but that the presence of O and C absorption edges at 23 and 44 Å could be powerful diagnostics of grain chemistry. Subsequently, Trümper and Schöenfelder (1973) discussed the effects of source variability on the temporal development of the scattered X-ray "halo." Alcock and Hatchett (1978) further suggested that the decay time of X-ray burst sources might be related to delays introduced by scattering from interstellar grains. Most recently, Norwell, Evans, and Bode (1983) have argued that transient halos might be detectable around eruptive sources such as dwarf novae.

The detection of scattered halos has had to await the development of imaging X-ray satellites such as *Einstein* and *EXOSAT*. Rolf (1980, 1983) presented evidence from *Einstein* imaging proportional counter (IPC) observations of the X-ray source GX 339−4 for a diffuse halo detected to $\sim 20'$ from the central source. Catura (1983) and Mauche and Gorenstein (1985), using similar techniques for *Einstein* high-resolution imager (HRI) and IPC data, respectively, found evidence for scattered halos in several X-ray bright, low Galactic latitude sources. In all these studies, halo surface brightnesses were derived by subtracting the energy-dependent point response function (PRF) of the telescope optics from the observed surface brightness distribution of point sources. One of the principal objections to this method is that it uses preflight calibration of the scattering properties of the mirror optics, which may well have changed during the mission. Another is that telescope scattering is a function of wavelength, so that inadequate knowledge of the source spectrum can lead to errors in the estimate of the telescope PRF.

In this paper, we apply a novel technique, utilizing source variability, for deriving the surface brightness distribution of a scattered halo. No assumptions are made regarding the PRF; indeed, this is found as a by-product of the technique. In § IV, the surface brightness distribution of the inferred halo of the bright, reddened X-ray source Cyg X-1 is compared to that derived theoretically using the grain size distributions by Mathis, Rumpl, and Nordsieck (1977).

II. SCATTERING THEORY

The scattering of X-rays by interstellar grains can accurately be described by the anomalous diffraction regime (see van de Hulst 1957). This regime holds for the wavelength range of the observations discussed below ($\sim$3–60 Å, 0.2–4 keV) and interstellar grains in the size range 0.005–0.4 μm radius. For these parameters, the conditions $|m-1| \ll 1$ and $x \gg 1$ must hold, where $x = 2\pi a/\lambda$ (a is grain radius, λ the wavelength of observation, and m the refractive index of the grain material). In the limit $\rho = 2x|m-1| \rightarrow 0$ (which implies no significant absorp-

tion within a grain), the simplifying Rayleigh-Gans approximation may be used, although here it was only called upon to check our anomalous diffraction results.

The surface brightness distribution of a source at a given wavelength is given by

$$I(\lambda, \alpha) = \int_{\theta} \int_{a} \frac{L(\lambda)}{4\pi} \frac{n_g(a)}{R \sin \alpha} \frac{d\sigma}{d\Omega} (\phi, a, \lambda) e^{-\tau(\lambda)} da \, d\theta \,, \quad (1)$$

where n_g is the number density distribution of grains, assumed to be distributed uniformly between source and observer. The source distance is R; θ, α, and ϕ $(= \theta + \alpha)$ are angles as defined in Figure 1, where ϕ is the scattering angle; L is the X-ray source luminosity; τ is the total optical depth (gas plus grains) from source to observer (from Brown and Gould 1970); and $d\sigma/d\Omega$ is the differential scattering cross section of a grain. This latter quantity is given, in the anomalous diffraction regime, by

$$\frac{d\sigma}{d\Omega} = a^2 x^2 |A|^2 \,. \quad (2a)$$

The value of A can be calculated from

$$\mathrm{Re}\,(A) = \sum_{n=1}^{\infty} (-1)^{n+1} \rho^{2n} 2^n \frac{n!}{(2n)!} J_{n+1}(z) \frac{1}{z^{n+1}} \,, \quad (2b)$$

and

$$\mathrm{Im}\,(A) = \frac{\rho}{y^2} \left(\frac{\pi y}{2}\right)^{1/2} J_{3/2}(y) \,, \quad (2c)$$

where $z = x\phi$, $y = (\rho^2 + z^2)^{1/2}$, and J_n are Bessel functions of order n. A fuller discussion of anomalous diffraction, and the derivation of equation (2), may be found in van de Hulst (1957, pp. 103–111, pps. 172–199). Numerical computation of $d\sigma/d\Omega$ shows that it increases with increasing wavelength, a property that will be of significance below. Refractive indices were taken from the approximation given by Hayakawa (1970) for carbon and silicate grains. These are accurate shortward of the absorption edges of O and C (23 and 44 Å) and can be used to model Cyg X-1, since most of its flux is observed at shorter wavelengths.

The key to detecting halos around variable sources is that there is a time delay, and consequent smearing, of scattered photons arriving at the observer because of different path lengths. Following Alcock and Hatchett (1978) this delay is of order

$$\Delta t \approx \frac{\phi^2 R}{8c} \,, \quad (3)$$

which with

$$\phi \approx 1/x \quad (4)$$

(Hayakawa 1970) gives

$$\Delta t \approx 0.22 \left(\frac{a}{0.25\ \mu\mathrm{m}}\right)^{-2} \left(\frac{\epsilon}{1\ \mathrm{keV}}\right)^{-2} \left(\frac{R}{2.5\ \mathrm{kpc}}\right) \mathrm{days} \,, \quad (5)$$

averaged over the scattered flux of photons of energy ϵ. Thus, for example, any scattered halo would be seen to persist for a considerable time after an eclipse or outburst of a source. Furthermore, such a halo would appear essentially nonvariable for a source which varies on a time scale of seconds.

III. DATA SELECTION AND REDUCTION

The *Einstein Observatory* provided the first opportunity to search for scattered X-ray halos using an imaging telescope. In this investigation, we selected archival images which might show time-invariant halos associated with intrinsically variable sources. Our first criterion in selecting such images was that they should have been made with the HRI. This instrument did not suffer from the background variations across an image or gain drift of the IPC. Next, we selected bright sources that were variable by virtue of either (i) outbursts, (ii) eclipses, or (iii) rapid intrinsic variability. The HRI data base contained no suitable sources in category (i), since these were either too faint or were not observed at a suitable time from outburst (a few days) for a halo to be detectable. In category (ii) the only bright source to be observed completely through eclipse was Her X-1 (McCray *et al.* 1982), although the observations were made with the objective-grating spectrometer (OGS) in place, reducing the nondispersed flux by a factor of ~ 4. Furthermore, since this object is ~ 3 kpc out of the Galactic plane, most scattering by dust will occur locally, with Δt a few hours. Thus, the halo flux might not persist through a substantial fraction of the eclipse. Of the bright sources in category (iii) showing rapid (a few seconds) variability, Cyg X-1 was chosen for detailed study, since it is well known to show short time scale variations well above those expected purely from Poisson statistics (Terrell 1972), and it was the subject of several long (> 1000 s), well-centered exposures. Table 1 gives details of the four Cyg X-1 images chosen for this study.

TABLE 1

CYGNUS X-1 HRI IMAGES

Exposure Date	Image Number	Effective Time (s)	Background[a]	V_c[b]	$\bar{s}_c$[b,c]
1978 Nov 20.....	H1	1280	1.10 ± 12%	362.3	48.37
1978 Nov 20.....	H12	1630	1.18 ± 13%	640.4	47.77
1979 May 17	H821	2990	1.37 ± 6%	491.5	100.5
1978 Nov 21.....	H1067	1180	1.40 ± 14%	70.5	42.12

[a] In cps arcsec^{-2} × 10^6.
[b] In 10 s bins.
[c] All values of $\bar{s}_c$ are for central 10″.

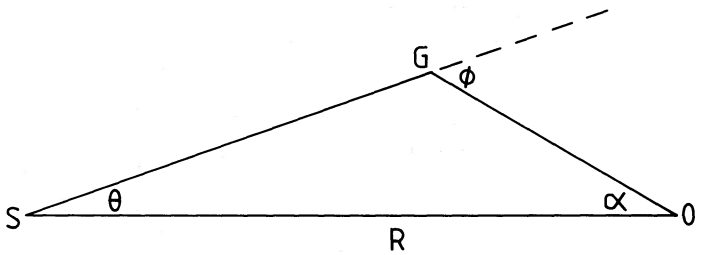

FIG. 1.—Geometry of the scattering. Source, grain, and observer lie at S, G, and O, respectively. Scattering angle is ϕ, and R is the source distance.

Before analyzing the images for the presence of any halo, each was inspected visually in order to determine whether there were any obvious background sources in the field. Then each image was subjected to an azimuthal binning program that determined the image center to an accuracy of $\pm 1''$. This same binning program was used to check that there were indeed no spurious sources in the field by comparing the counts in each of eight azimuthal bins at increasing radii from the central source. In no case was variation above that expected purely from counting statistics found.

The background was estimated by summing the counts in several bins well away from the central source. Care was taken to avoid part of any bin falling off the edge of the image. In each case the background rate was consistent with normal in-flight experience.

Images H1, H12, H821, and H1067, of Cyg X-1 were binned radially from the central source in annuli tending to increase in width at larger radii (to compensate to some extent for the fall in counts away from the central source). Each spatial bin was then divided into temporal bins. The variance V in each radial bin was than calculated from

$$V = \frac{1}{N-1} \sum_{i=1}^{N} (s_i - \bar{s})^2 , \tag{6}$$

where N is the total number of temporal bins and s_i is the number of counts in the ith temporal bin. For each image, the total variance in the central 10″ bin significantly exceeded the mean counts, $\bar{s}$, in that bin, reflecting the intrinsic variability of Cyg X-1 (see Table 1).

Because the halo is time invariant, we can discriminate between halo and central source contributions to the image. The observed flux contains both time-variant and time-invariant contributions, plus Poisson noise. The intrinsically variable contribution is the central source signal, which has been scattered by the telescope optics to an off-axis position as specified by the PRF. Since there is no time delay in this process, the PRF flux tracks the central signal. The halo flux is the sum of scatterings with a wide range, Δt, of time delays, so that it can be regarded as constant. In the central bin of the image, the halo is negligible; the observed variance, V, is purely the sum of the intrinsic source variance, V_s, and the Poisson variance, $\bar{s}$. The value of V_s thus calculated is applied to the analysis of the annular bins.

In any bin at a radial distance α arc seconds from this central bin, the total count rate will be the sum of the background counts, $B(\alpha)$; the telescope off-axis response to the central source, which is the central bin signal times the quantity $r(\alpha)$, equivalent to the PRF multiplied by the ratio of the area of the bin at radius α to that of the central bin; and any contribution from the scattered halo $H(\alpha)$; i.e.,

$$H(\alpha) = \bar{s}(\alpha) - r(\alpha)\bar{s}_c - B(\alpha) . \tag{7a}$$

The intrinsic variance in any radial bin is just the difference between the observed variance in that bin and the mean counts, viz.,

$$V_s(\alpha) = V(\alpha) - \bar{s}(\alpha) . \tag{7b}$$

With the assumptions given above, any variability over and above Poisson noise, seen in a bin at radius α, can only be due to the off-axis response to the varying central source. The value of $r(\alpha)$ can simply be determined from

$$r(\alpha) = [V_s(\alpha)/(V_s)_c]^{1/2} , \tag{7c}$$

where $(V_s)_c$ is the source variance measured in the central bin (see Sutherland, Weisskopf, and Kahn 1978). Thus, all the variables on the right-hand side of equation (7a) are defined, and the value of the halo contribution to the count rate in a given radial bin can be found.

To test the validity of this analysis technique, a simulated image of Cyg X-1 was constructed. The shot noise nature of the source was simulated using a Poisson noise generator giving randomly spaced shots with a mean rate of 1 s^{-1} and an exponential decay for each shot with a time constant of 0.5 s. The mean source flux was then normalized to the mean count rate in the central bin of one of the observed images. The counts in any temporal bin for a spatial bin at radius α were then found by multiplying the central source counts at the relevant time by a simulated PRF. Contributions to the counts in any bin were also made by an assumed background rate and the flux from a simulated halo. Both the PRF and halo were taken from Catura (1983). Finally, Poisson noise was added to each signal.

The simulated image was then analyzed in the same way as the Cyg X-1 data; i.e., the variance and mean were found in each radial bin, and $r(\alpha)$ and $H(\alpha)$ were determined using equations (7a)–(7c). The results of this analysis are shown in Figure 2 for the particular case of a shot noise source with a fall to half-mean flux 1300 s into a 1950 s exposure. It can be seen that this method returns the assumed PRF within the calculated errors and thus gives the surface brightness distribution of the model halo. For one annular bin (240″–300″), the observed variance $V(\alpha)$ was exceeded by the mean count rate $\bar{s}(\alpha)$; i.e., statistical fluctuations were such that there is no excess variability to ascribe to the central source. In this case, an upper limit can be derived for the PRF, implying a lower limit to the halo flux, $H(\alpha)$. An upper limit is calculated by assuming that all the flux above background is from the halo. Both limits are plotted. As a last check, a simulated image with no halo present was analyzed. Reassuringly, no spurious halo was detected. This method also succeeded in deriving accurate halo fluxes for simulated periodic central source light curves.

IV. RESULTS AND DISCUSSION

The analysis given in § III was applied to all four of the images of Cyg X-1. A significant contribution from a constant off-axis source, interpreted to be a scattered halo, was found in each image. Typically, at a radius $\alpha \approx 2'$, $\sim 70\%$ of the observed counts are from the X-ray halo, while only $\sim 30\%$ from the telescope PRF. For the three longer duration exposures, the halo contribution could be detected to $\lesssim 5'$ from the source. We may note that the observed halo exceeds instrumental background for all $\alpha \lesssim 5'$. In the case of H1067, not only were there fewer photons in the image, but the source seemed to have rather lower intrinsic variability. Thus, the halo could not be mapped as well as for the other exposures. Exposure H1 included a filter change part way through the exposure. The additional "variability" in the source would lead to underestimation of any halo flux. We may note here that the inclusion of any additional variability such as this *cannot give rise to a spurious halo*, but will serve only to diminish the derived flux. We may also note that there is no observed energy dependence in the shot noise behavior (Priedhorsky, *et al.* 1979). Results from H12 and H821 will be discussed below.

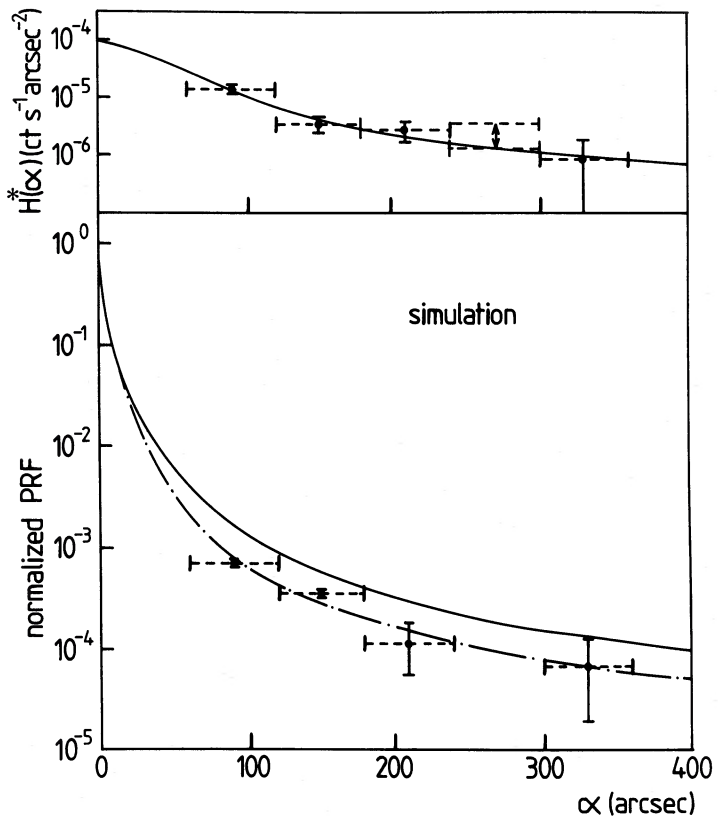

FIG. 2.—Results of analysis of simulated image. Lower portion of figure shows the point response function (*chain dashed line*) and total surface brightness distribution (*solid line*), including scattered halo. Upper portion shows input surface brightness distribution of halo. Points shown were extracted from simulated image using analysis of § III. $H^*(\alpha)$ is just $H(\alpha)$ divided by bin area and sample time. Vertical error bars are 95% confidence limits. Horizontal error bars simply denote radial bin size. See text for explanation of limits on 240–300″ bin.

Figures 3*a* and 3*c* show results for H12 and H821, respectively. The derived halo in H821 was brighter than that in H12 by a factor of ~ 2, approximately in keeping with the ratio of central source fluxes, as is indicated by the normalized points shown in Figures 3*a*–3*c*. The dashed line in Figure 3*a* is the scattered halo derived by Catura (1983) for GX 17+2. It can be seen that the halo profiles are very similar. The major difference is that the halo of GX 17+2 represents $\gtrsim 20\%$ of the observed central source flux, whereas in H12 the fraction is $\gtrsim 12 \pm 4\%$. This discrepancy may arise from the fact that the path lengths through dust in the Galactic plane, d_d, are given as 4.6 kpc for GX 17+2 (Catura 1983) and $2.5 < d_d < 3$ kpc for Cyg X-1 (Bregman *et al.* 1973). Indeed our results for Cyg X-1 are consistent with the relationship of halo fraction to d_d (or A_v) found by Mauche and Gorenstein (1985). The lower limit on scattered halo fraction results from halo flux at $\alpha \lesssim 30''$ not being accounted for in the summation. The theoretical modeling outlined below tends to suggest that the underestimation is $\sim 30\%$.

As a test of the consistency of the halo interpretation of the residual flux in the Cyg X-1 images, a scattering model was constructed based on equation (1). Ideally, one requires a knowledge of the X-ray flux distribution throughout the HRI energy range (but particularly at low energies) at the time of the observations. While some information may be available from the monitor proportional counter (MPC), this is not particularly helpful from our point of view because of its low sensitivity at energies $\lesssim 2$ keV. Accordingly, the unattenuated spectral luminosity was taken from Priedhorsky *et al.* (1979) as

$$L(\lambda) = A(\lambda^2 + f\lambda^{-1.6}) \text{ ergs s}^{-1} \text{ Å}^{-1} . \quad (8)$$

The factor $f(=4850)$ normalizes the hard and soft spectral components and is such that these have equal intensity at 10.6 Å. Priedhorsky *et al.* (1979) present strong evidence that the column density, based on measured E_{B-V} for Cyg X-1, is $N_{\rm H} = 7 \times 10^{21}$ cm^{-2}. The corresponding cutoff in energy E_a is 1.2 keV. For images H12 and H821, A was determined to be 7×10^{32} and 1.5×10^{33}, respectively, for a distance of 2.5 kpc, normalized to the observed HRI count rate for this incident spectrum. During all these observations, Cyg X-1 was in the normal low state (Priedhorsky *et al.* 1983).

The grain size distribution for olivine (O1) and graphite (C) grains was taken from fits to the UV–IR extinction curve by Mathis *et al.* (1977), which is the most rigorous fit to the observational data presently available. Thus,

$$\log n(a) = -15.24 - 3.5 \log (a/1\ \mu\text{m}) \quad (0.005 < a < 0.25\ \mu\text{m}) ,$$

$$\log n(a) = -15.21 - 3.5 \log (a/1\ \mu\text{m}) \quad (0.025 < a < 0.25\ \mu\text{m}) , \quad (9)$$

where $n(a)$ is in units of particles per H atom μm^{-1}. Mathis *et al.* assume that the grain density does not violate standard cosmic abundances. The exponent of -3.5 in the power-law size distribution has subsequently been shown by Biermann

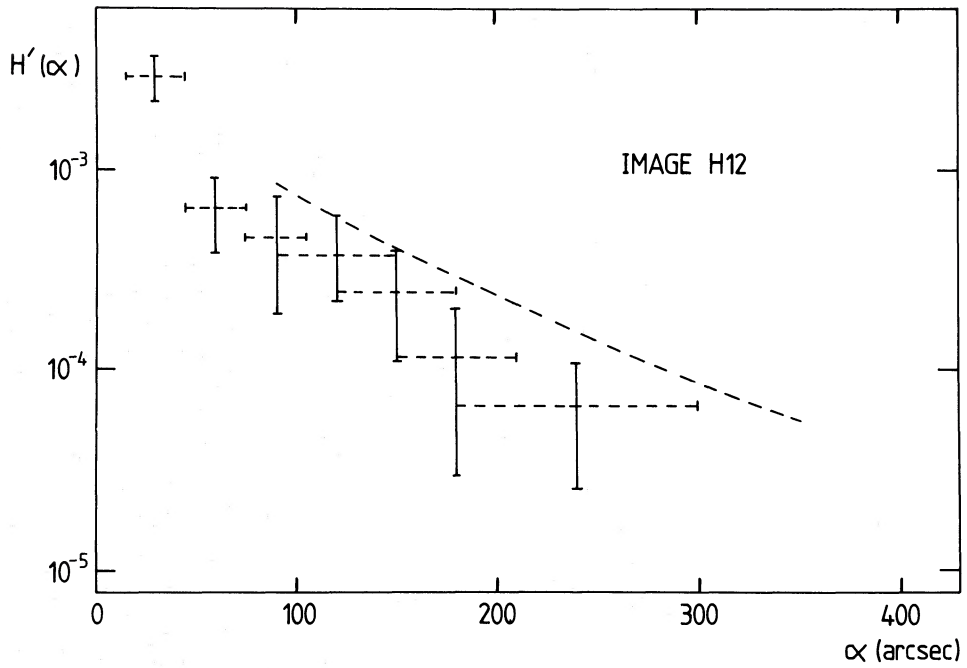

FIG. 3*a*.—Extracted halo of Cyg X-1. $H'(\alpha)$ is halo surface brightness, normalized to count rate in central 10″ bin, derived for image H12 using analysis in § III. Error bars are as in Fig. 2. Dashed line is normalized halo for GX 17+2 (Catura 1983).

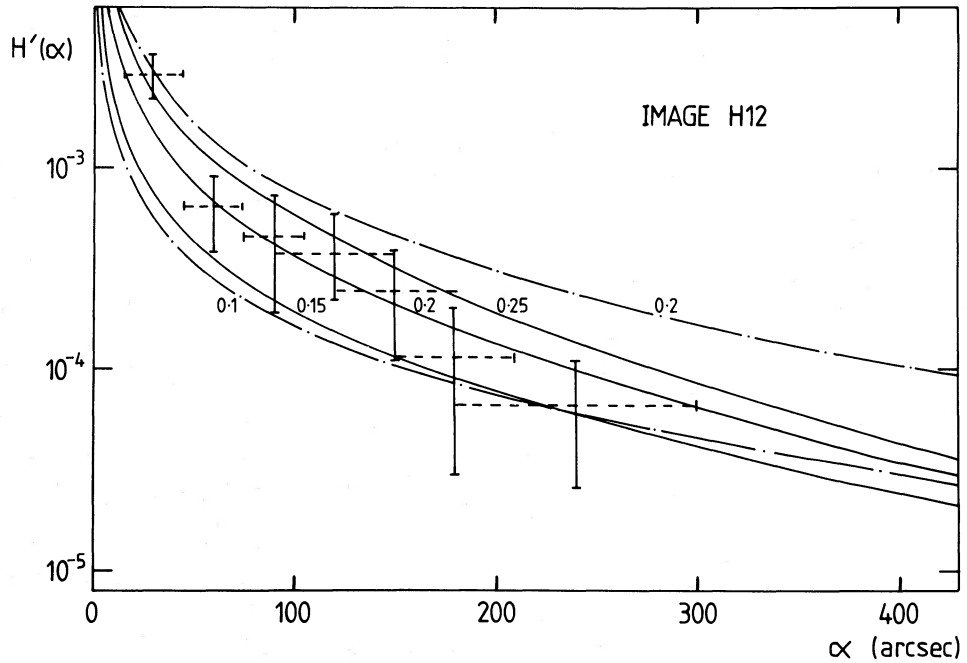

FIG. 3*b*.—As Fig. 3*a*, except results of scattering model using Mathis *et al.* (1977) grain size distributions, are shown. Chain dashed curves are results of a two-component source spectrum as input, whereas solid curves are results of model with only a hard component. Numbers beside these curves are maximum grain radius in microns used in model.

and Harwit (1980) to be a natural consequence of grain-grain collisions in red giant atmospheres. A value of 1 H atom cm^{-3} was taken from $N_H = 7 \times 10^{21}$ cm and $d = 2.5$ kpc. The photon fluxes at each wavelength, arising from numerical integration of equation (1), were then folded though the HRI effective area during integration over the HRI wavelength range. The effective area quoted by Giacconi *et al.* (1979) includes only photons detected within 6″of the central source. Based on our derived PRF, the effective area for an extended (a few arc minutes) source is ~1.75 times greater; this correction was thus applied in our calculations.

The chain-dashed lines in Figures 3*b* and 3*c* show the resulting surface brightness distributions for the two-component source spectrum, the above distance and column density, and the Mathis *et al.* grain model of equation (9). It can be seen from these figures that the interpretation of the

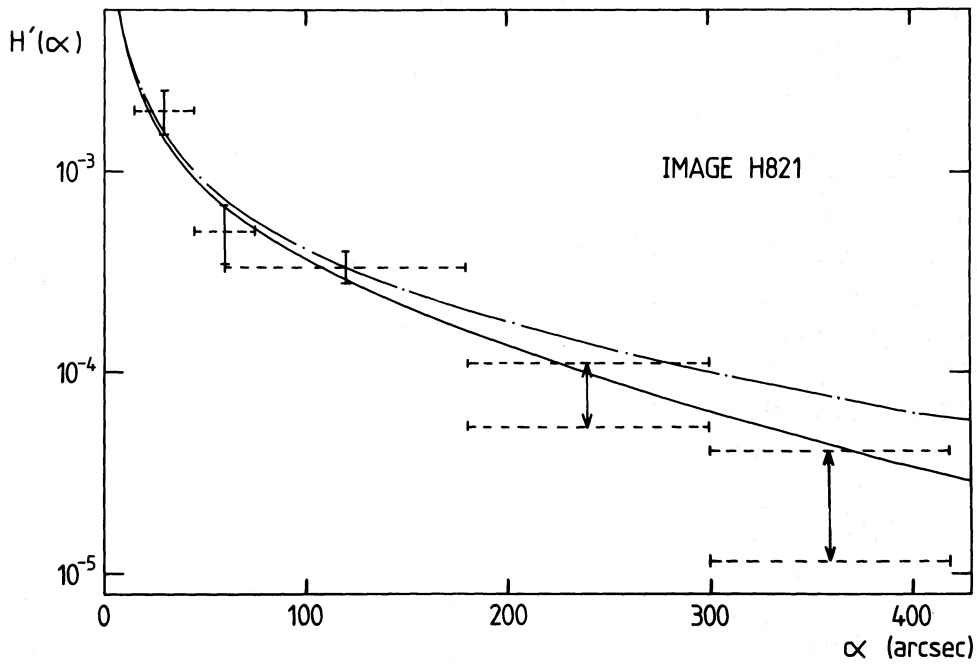

FIG. 3*c*.—Similar to Fig. 3*b*, except that these results are for image H821 of Cyg X-1. The 180″–300″ bins were analyzed in the same way as the 240″–300″ bins of Fig. 2. Chain-dashed curve denotes two-component model with $a_{max} = 0.15$ μm, and solid curve denotes model with only a hard component and $a_{max} = 0.2$ μm.

nonvariable component as a scattered halo is not unreasonable, but that an upper limit on grain size of 0.25 μm would give far too high a resultant halo flux. The results suggest $0.1 < a_{max} < 0.2$ μm, with the best fit to the data being $a_{max} \approx 0.15$ μm. However, all values of a_{max} produce a halo which is less centrally peaked than that observed. This can be seen particularly in Figure 3*c* where the 0.15 μm model exceeds all the upper limits at large values of α.

To diminish halo surface brightness at large α, one needs to decrease the typical value of ϕ. From equation (4), this may be achieved either by decreasing the number density of small grains, by making the exponent in the size distribution less than 3.5, or by decreasing the number of soft X-ray photons. The solid lines in Figures 3*b* and 3*c* show the results of the latter alternative, where the soft component of the source spectrum has been removed, and the spectrum renormalized to the observed HRI count rates. As can be seen, the model halo is more centrally peaked, and $0.15 < a_{max} < 0.25$, with an improved fit to the data for $a_{max} = 0.2$ μm. The fact that larger values of a_{max} result reflects the tendency of $d\sigma/d\Omega$ to increase with increasing wavelength (a tendency masked by the apparent complexity of equations [2a]–[2c]). Furthermore, that the present results are so sensitive to a_{max} is not surprising. In equation (2a), $d\sigma/d\Omega$ is shown to be very sensitive to a. Indeed, in the region of parameter space where the Rayleigh-Gans approximation is valid, $d\sigma/d\Omega$ is approximately proportional to a^6 (Catura 1983). These results demonstrate the considerable potential of X-ray scattering as a probe of the larger grain population of interstellar dust. This is precisely where the UV–IR extinction becomes gray and therefore not very helpful.

In addition to the effects of uncertainties in the source X-ray spectrum, we have explored the effect of uncertainty in source distance and, hence, in N_H and L. For values of d in the range $2.1 \lesssim d \lesssim 2.9$ kpc, corresponding to $6 \times 10^{21} \lesssim N_H \lesssim 8 \times 10^{21}$ cm^{-2}, halo flux changed approximately in proportion to the distance (i.e., optical depth) change, as might be expected (Hayakawa 1970).

Despite the uncertainties in the various parameters, it is clear that the surface brightness distribution of the nonvariable component of the Cyg X-1 images is consistent with an interpretation in terms of scattering by interstellar dust. Furthermore, it appears that the upper limit of 0.25 μm on grain size, deduced by Mathis *et al.*, is confirmed. However, the application of the method to images with better spectral and temporal resolution could refine this upper limit considerably.

V. CONCLUSIONS

The analysis described above demonstrates conclusively the observational reality of X-ray scattering by interstellar grains. The results confirm the halo observations of Rolf (1980), Catura (1983), and Mauche and Gorenstein (1985). They are also not inconsistent with the fits to the UV–IR extinction curve of Mathis *et al.* (1977).

Future observations would ideally define the source light curve over several days prior to the imaging so that long-term changes would be accounted for and would also incorporate simultaneous spectral information, particularly at low energies. Although these conditions are not met by the data available at present, we may tentatively conclude that there must be a very sharp cutoff in the grain number density for large ($a \gtrsim 0.25$ μm) grains.

The potential of X-ray scattering observations to the probing of the dust component of the interstellar medium cannot be overemphasized. It is, however, ironic, and a testament to the inherent difficulties in detecting such effects, that evidence for X-ray halos has only now come to light from some of the first images to be taken with the first instrument capable of making these detections.

This work was performed under NASA grant number H-705 73B, with additional support from the US Department of Energy and the UK Science and Engineering Research Council. The authors are very grateful to the staff of the *Einstein Observatory* at the Center for Astrophysics for their help in the data acquisition. Particular thanks must go to F. D. Seward. We also held fruitful discussions with R. Epstein on the data analysis. G. A. N. acknowledges partial travel support from the University of Keele.

REFERENCES

Alcock, C., and Hatchett, S. 1978, *Ap. J.*, **222**, 456.
Biermann, P., and Harwit, M. 1980, *Ap. J. (Letters)*, **241**, L105.
Bregman, J., Butler, D., Kemper, E., Koski, A., Kraft, R., and Stone, R. P. 1973 *Ap. J. (Letters)*, **185**, L117.
Brown, R. L., and Gould, R. J. 1970, *Phys. Rev. D*, **1**, 2252.
Catura, R. C. 1983, *Ap. J.*, **275**, 645.
Giacconi, R., *et al.* 1979, *Ap. J.*, **230**, 540.
Gursky, H., *et al.* 1980, *Ap. J.*, **237**, 163.
Hayakawa, S. 1970, *Progr. Theor. Phys.*, **43**, 1224.
Martin, P. G. 1970, *M.N.R.A.S.*, **149**, 221.
Mathis, J. S., Rumpl. W., and Nordsieck, K. H. 1977, *Ap. J.*, **217**, 425.
McCray, R. A., Shull, J. M., Boynton, P. E., Deeter, J. E., Holt, S. S., and White, N. E. 1982, *Ap. J.*, **262**, 301.
Mauche, C. W., and Gorenstein, P. 1985, *Ap. J.*, submitted.
Norwell, G. A., Evans, A., and Bode, M. F. 1983, *Nature*, **303**, 49.
Overbeck, J. W. 1965, *Ap. J.*, **41**, 864.
Priedhorsky, W. C., Garmire, G. P., Rothschild, R., Boldt, E., Serlemitsos, P., and Holt, S. 1979, *Ap. J.*, **233**, 350.
Priedhorsky, W. C., Terrell, N. J., and Holt, S. 1983, *Ap. J.*, **270**, 233.
Rolf, D. P. 1980, Ph. D. thesis, University of Leicester.
———. 1983, *Nature*, **302**, 46.
Sutherland, P. G., Weisskopf, M. C., and Kahn, S. M. 1978, *Ap. J.*, **219**, 1029.
Terrell, N. J. 1972, *Ap. J. (Letters)*, **174**, L35.
Trumper, J., and Schoenfelder, V. 1973, *Astr. Ap.*, **25**, 445.
van de Hulst, H. C. 1957, *Light Scattering by Small Particles* (New York: Wiley).
Whittet, D. C. B. 1981, *Quart. J.R.A.S.*, **22**, 3.

M. F. Bode: Department of Astronomy, University of Manchester, Oxford Rd., Manchester M13 9PL, England, UK

A. Evans and G. A. Norwell: Department of Physics, University of Keele, Keele, Staffordshire ST5 5BG, England, UK

W. C. Priedhorsky: ESS-9, MS D436, Los Alamos National Laboratory, Los Alamos, NM 87544